

Biosynthesizing *Cassia fistula* Extract-Mediated Silver Nanoparticles for MCF-7 Cell Lines Anti-Cancer Assay

Rija Abaid,[◆] Maria Malik,[◆] Muhammad Aamir Iqbal,^{*} Mariam Malik, Zubeda Shahwani, Taha Zaid Ali, Kareem Morsy, Rey Y. Capangpangan, Arnold C. Alguno, and Jeong Ryeol Choi^{*}



Cite This: *ACS Omega* 2023, 8, 17317–17326



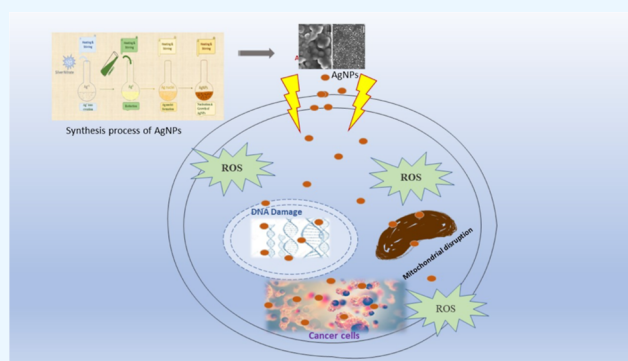
Read Online

ACCESS |

Metrics & More

Article Recommendations

ABSTRACT: The unique consequence of green synthesis is that the mediator plant is able to release chemicals that are efficacious as reducing as well as stabilizing agents. In this work, the fruit pulp and leaf essences of *Cassia fistula* have been used to manufacture silver nanoparticles through the green synthesis technique. The sculpturing of nanoparticles was accomplished by utilizing the reduction phenomenon that ensued due to the reaction between plant essences and the precursor solution. These biosynthesized silver nanoparticles were examined, where we used scanning electron microscopy, UV–vis spectroscopy, and X-ray diffraction techniques as means to analyze the structure, optical properties, and crystalline behavior, respectively. The absorption spectra for fruit and leaf extracts obtained from the UV–vis analyses peaked at 401 and 397 nm, and these peaks imply the appearance of optical energy gaps of 2.12 and 2.58 eV, accompanying spherical shapes of particles with diameters in the ranges of 12–20 and 50–80 nm, respectively. These silver nanoparticles together with the adopted green technique have a vast array of applications, specifically in the biomedical realm. In particular, they are being used to treat several diseases and are manifested as strong anti-tumor agents to medicate MCF-7 breast cancer cell lines in order to minimize the cell growth rate depending on their concentrations.



1. INTRODUCTION

Nanotechnology can be spelled out as the manipulating and fabrication of materials at the atomic scale to enhance their properties significantly more than those of bulk materials.¹ Nanoparticles (NPs), having different appearances and sizes varying between 1 and 100 nm, are nowadays in the practice of being manufactured in laboratories because of their extensive usage in a variety of industries. Presently, top-down and bottom-up approaches are being widely employed for NP chemical and physical synthesis, but the adoption of precarious and unsafe chemicals is their snag.^{2,3} Meanwhile, nanotechnologists have discovered a more advantageous method of producing NPs, which is popular because it is user-friendly, does not require complex instruments, and raises relatively low environmental toxicity.⁴ This method is known as “Green Synthesis,” which correlates plants with nanotechnology. It has caught the limelight due to the use of safer chemical processes.⁵ Other synthesis techniques, for example, chemical or physical ones, being used for the fabrication of nanosized particles call for the use of reducing and capping agents, as well as stabilizing agents in the form of additional complex and toxic chemicals, but this is not the case in green synthesis because such chemicals that serve as the reducing agents and

stabilizing agents are already present in the parent plant.⁶ NPs have been told to be green synthesized by employing different parent plants^{7,8} and making use of their seeds,⁹ leaves,¹⁰ flowers,¹¹ and stem bark¹² as NP mills. Silver NPs synthesized using *Moringa oleifera* leaf essence,¹² zinc oxide NPs treated by a fruit extract of *Capsicum annuum*,¹³ platinum nanosized particles made using date essence,¹⁴ ferris oxide NPs produced using *Tabebuia aurea* leaf extract¹⁵ can be employed for a range of biomedical applications. Furthermore, cobalt oxide NPs from *Muntingia calabura*,¹⁶ as well as hydroxyapatite NPs from eggshells,¹⁷ can be applied to the dye and photocatalysis process. Many others besides them have been suggested so far, which serve in the efficient synthesis of NPs by employing eco-friendly green synthesis methods for not only metallic NP synthesis but for ionic ones as well.

Received: April 3, 2023

Accepted: April 21, 2023

Published: May 1, 2023





Figure 1. Steps involved in the preparation of *C. fistula* leaves extract.

The most noteworthy feature of NPs is their increased reactivity, and the reason is their higher surface-to-volume ratio, which reveals the secret of their applications being dependent on their size. Nowadays, the more effective NPs are metal NPs, like Ag, Zn, and Au, although the more significant role in biological fields is played by AgNPs. Biology-based methods act as the factories of NPs, especially when we require NPs for enhanced enzyme activity, and other aspects like cell growth and genetic properties of organisms are of interest.¹⁸ Biosynthesized metallic ZnO NPs, fluctuating in size between 25 and 40 nm, have also been reported to be fabricated using the gel from the *Aloe barbadensis* plant.¹⁹ Flower extract of *Cassia alata* was also used as a strong reducing and capping agent to manufacture CuO nanosized particles, wherein the phytochemicals, such as flavones, sugars, aldehydes, ketones, and amides, were reported to be the main ingredients that played their role in the biosynthesis of NPs through reduction mechanisms.²⁰ *Cassia fistula* (*C. fistula*) contains a wide variety of antioxidants, for example, terpenoids, flavonoids, alkaloids, phenolic compounds, tannins, saponins, anthocyanosides, carbohydrates, proteins, steroids, cardiac glycosides, and phlobatannins. Owing to the action of these antioxidants, silver ions are effectively reduced into silver NPs.²¹ Herein, flavonoids are the main ingredient responsible for antioxidant owing to their tautomeric reactions to convert the enol-form into the keto-form by releasing the reactive hydrogen atom which converts ions into metallic particles.²² Moreover, sugars, such as glucose and fructose present in plant extracts contribute to managing the size and shape of the synthesized NPs, while the mono-dispersity of nanosized particles is given by fructose.²³ Protein in plant extracts contains an amino acid functional group, which is helpful for the reduction of metallic ions. Moreover, alkaloids, phenols, and flavones also enhance the agglomeration of metallic atoms, which is required in synthesizing metallic NPs. *C. fistula* plant parts are also reported to be used as a cure for many deadly diseases, including antiparasitic activity, laxative activity, hypoglycemic activity, antitumor activity, anti-infertility activity, antifungal activity, and antioxidant activity.²⁴ Different plant parts have different compositions and different properties. Rhein, which is an anthraquinone derivative and is a major fighter against tumor and inflammatory cells, was observed in the fruit pulp of

C. fistula, and it was investigated to confirm its high toxicity against cancer cell lines.^{25,26} Despite this, the leaves of the *C. fistula* plant are rich in anthraquinones, phenolics, and flavonoid compounds,²⁷ which could also prove to be promising agents against the mentioned deadly diseases.

The current investigation has the goal of exploring the synthesis of AgNPs utilizing the biosynthesis technique, making use of the leaf and fruit extracts of the *C. fistula* plant to point out their strength in the biological field. According to our understanding, it is the first-mentioned study that, regarding the *C. fistula* and leaf extracts' potential for anticancer treatments, delivers us with clear data on the fruit and leaf essences for size-dependent applications. This detailed work bubbled out the efficient anticancer efficacy of this plant's extracts without using any chemical products and keeping the sterility of the green-synthesized AgNPs. For the very first time, the anticancer efficacy of synthesized AgNPs at different concentrations between 10 and 100 $\mu\text{g}/\text{mL}$ was examined.

2. MATERIALS AND METHODS

2.1. Materials and Equipment. Freshly cut *C. fistula* fruits and green leaves were collected from the departmental garden of the University of the Punjab, Lahore, Pakistan. The obtained plant parts were washed, dried, and ground into a fine powder. Silver nitrate solution (AgNO_3) was the only chemical used for this NP synthesis procedure, which was bought from Sigma-Aldrich Inc. Lahore, Pakistan, with a purity of 99.9%. The deionized water used in the synthesis procedure was made at the departmental lab. The instruments used in this study included a magnetic stirrer, magnetic bits, beakers, a hot plate, a weight balance, a micropipette, and Petri dishes. All the experiments were performed under ambient conditions.

2.2. Method Illustration. The method followed to synthesize the required NPs is categorized into three parts as (I) leaves extract and fruit extract preparation, (II) precursor solution preparation, and (III) NP synthesis.

2.2.1. Leaves Extract Preparation. The freshly cut *C. fistula* leaves were, first of all, washed with fresh water 2–3 times to avoid any inconsistency in results. Cleaning was followed by a drying step in a dark environment (i.e., with no sunlight). The desiccated leaves were pulverized exquisitely by manipulating them with a grinder. 5 g of crushed leaves powder was mixed in



Figure 2. Steps involving the preparation of *C. fistula* fruit (pulp) extract.

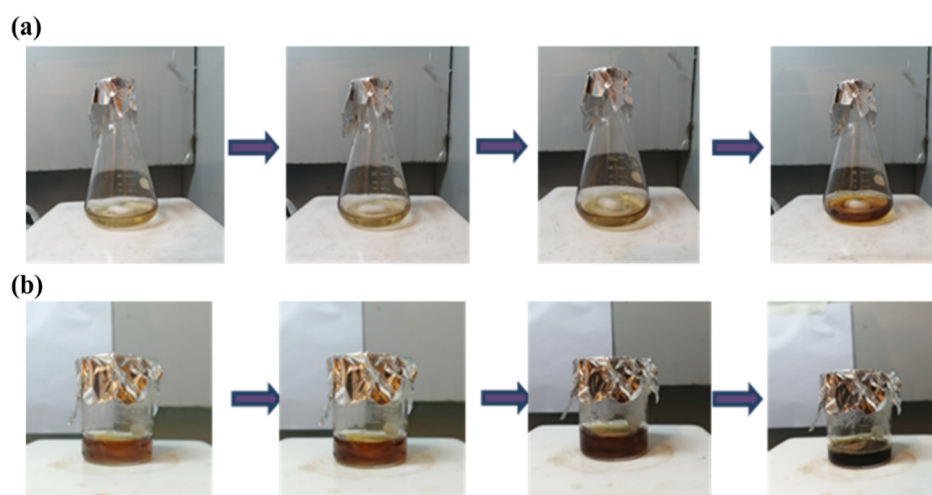


Figure 3. Steps involving the preparation of *C. fistula* plant: (a) leaves-mediated NPs, and (b) fruit-mediated AgNPs.

100 mL of deionized water to muster the essence from leaves, followed by boiling this solution at 700 rpm for 35 min using a hot plate. This step was followed by filtering using Whatman filter paper no. 1. The synthesis of the leaf extract in the series of steps followed is shown in Figure 1.

2.2.2. Fruit Extract Preparation. The *C. fistula* pods were peeled, cut, and the yellow-colored fruit extracted, which was rinsed 2–3 times before being placed in the dark for nearly 15 days until fully dried and ready to be ground with a grinder. For the extract preparation, 2 g of dark brown-colored powdered pulp was weighed and put in 50 mL of deionized water for 24 h. After that, it was heated at 60 °C and 600 rpm for 30 min. The final fruit essence was obtained by the filtration of the solution using Whatman filter paper no. 1. A dark brown solution was obtained through the procedure illustrated in Figure 2.

2.2.3. Precursor Solution Preparation. An amount of 0.0169 g of AgNO_3 powder was mixed in 100 mL of deionized water to make a 100 mL solution of 1.0 mM AgNO_3 which was used as a precursor for *C. fistula*-treated AgNPs leaves and fruit extracts.

2.2.4. *C. fistula* Leaf Extract-Mediated AgNPs. *C. fistula* leaf extract-treated AgNPs were made by dropping 1 mL of leaf

essence into 18 mL of the boiling silver nitrate precursor solution and boiling for another 25–30 min at 600 rpm. As shown in Figure 3a, the surface plasmon resonance (SPR) effect caused the change in color from light yellow to light brown and then appeared to be dark reddish brown, representing a change in pH. This indicates the formation of dark reddish brown-colored AgNPs.²⁸ These synthesized AgNPs were then kept at 4 °C for further characterization.

2.2.5. *C. fistula* Fruit Extract-Mediated AgNPs. To synthesize *C. fistula* fruit-mediated AgNPs, we boiled 18 mL of precursor solution in a beaker and then added 2 mL of *C. fistula* fruit extract dropwise into the boiling precursor solution. This solution was then further boiled for almost 30–35 min at 600 rpm, after which the color was observed to be transforming from crystal clear to light brown and finally to dark brown. The SPR effect caused the color to vary from light yellow to finally dark reddish brown through different stages, presenting a change in pH and pointing to the synthesis of dark reddish brown colored AgNPs,²⁸ which were then kept at 4 °C for further procedures.

Figure 3a,b shows the step-by-step color transformations during the synthesis of NPs. These AgNPs synthesized using the leaf and fruit essence of *C. fistula* were examined using

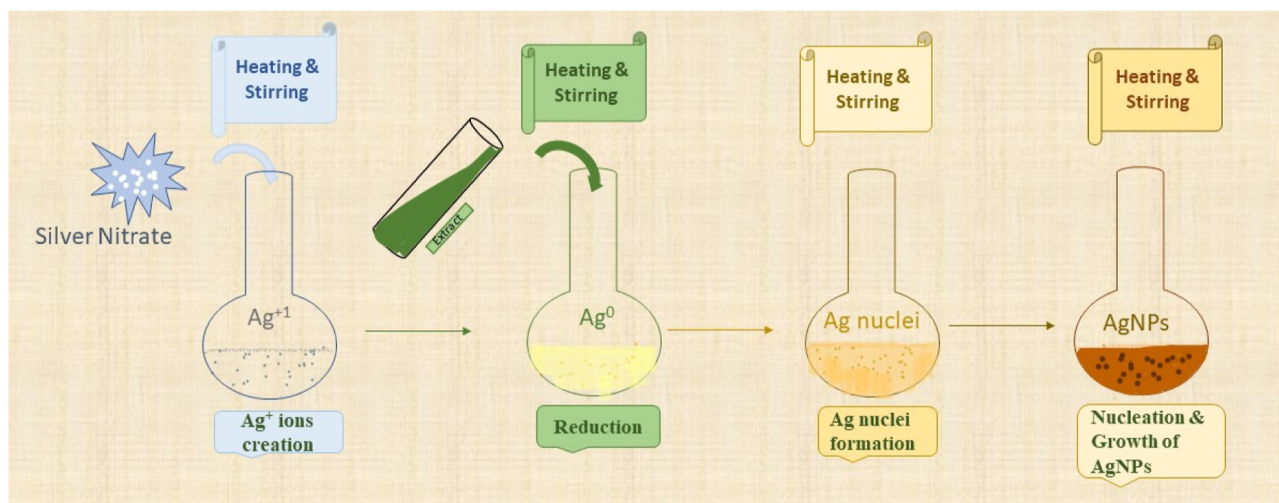


Figure 4. Schematic for the fabrication of green-synthesized NPs.

basic characterization techniques, including scanning electron microscopy (SEM, S3400N, Hitachi Analysis Machine, Tokyo, Japan), X-ray diffraction (Bruker D8 Advance Diffractometer, Bremen, Germany), and UV–visible spectroscopy (Shimadzu UV-1800, Shimadzu Corp., Kyoto, Japan).

2.3. Synthesis Mechanism of Silver NPs. The biosynthesis technique bestows us with another origin to synthesize AgNPs, which possess some noteworthy physical and optochemical attributes that are predominant in bio-nanotechnology,^{29–31} in which reducing agents are the plant extracts themselves.³² Upon the addition of plant extracts to the precursor solution, a reduction process occurred, providing us with the required AgNPs.³³ Figure 4 shows a schematic mechanism of silver NP preparation in which AgNO_3 powder was added to deionized water, which was colorless. This solution was passed through boiling and stirring on a hot plate while boiling, followed by the addition of *C. fistula* leaf or fruit essence into a beaker. This essence solution played the role of a reducing agent, which in this case converted Ag^{+1} ions into Ag^0 upon continuous heating accompanied by stirring on a hot plate. This step is the bottom of silver NPs nucleation, which can be observed by the variations in the solution's color. Moreover, the additional heating sped up the processes of nucleation and growth of the particles, which consequently provided us with the AgNPs certified by the color of the product solution. In this green synthesis, reducing agents such as phenolic compounds, and so forth found in the extracts were the root cause behind the reduction of Ag^{+1} ions to Ag^0 particles, so the color revolution was considered a reduction process.³⁴ Moreover, by adjusting the quantities of plant extract, precursor solution, and temperature, the desired size of the produced particles can be easily obtained.³⁵

2.4. Protocols for Anti-Cancer Assay. **2.4.1. MCF-7 Cell Line Culture.** The cancer cell line of the human breast, also named as the MCF-7 cell line, was picked up from the cell collection section of the Biological Sciences department of the University of the Punjab, Lahore, Pakistan. For the culturing of the cell line, Dulbecco's modified Eagle's medium (Gibco) was used, which was further augmented with 10% fetal bovine serum (FBS) (Gibco) along with 1% penicillin–streptomycin (Gibco) while maintaining in an incubator at 37 °C. The procedure applied for cultivating cells making use of trypsin–EDTA was standard trypsinization.

2.4.2. MTT Assay. The cell viability study was accomplished with the MTT (3-[4,5-dimethylthiazol-2-yl]-2,5-diphenyltetrazolium bromide) reduction assay to estimate the cytotoxicity of Ag NPs and the plant extract. First, a plate having 96-wells with a density of 5×10^3 cells per well was taken, and MCF-7 cells were seeded on it and kept for 24 h in the EMEM concentration of 200 μL with 10% FBS, allowing the cells to attach and grow on it. The next step involved the removal of media and replacing it with a suspension of silver NPs, varying in their concentration from 10 to 100 $\mu\text{g}/\text{mL}$. Each of these concentrations was used to seed four wells at the minimum and then stored in an incubator for another 48 h. After the addition of MTT, the cells were stored in an incubator for another 4 h at the setting temperature of 37 °C, followed by removing the medium. Furthermore, each well was loaded with 200 μL of dimethyl sulfoxide. The cell viability percentage was computed by applying the following formula given in eq 1, subjected to an optical density (OD) value from the spectrometer.²⁹

$$\text{Cell viability (\%)} = \left(\frac{\text{OD of sample}}{\text{OD of control}} \right) \times 100 \quad (1)$$

3. RESULTS AND DISCUSSION

3.1. X-ray Diffraction Analysis. The XRD technique was used for the structural investigations of the as-synthesized NPs to examine the purity of the material, its crystal composition, lattice parameter, crystallite size, as well as crystal defects.^{36,37} The XRD technique is considered as a non-destructive method working on a coherent scattering mechanism, which works on a procedure wherein the sample material is rotated at varying angles to record the reflected X-rays strength at the rotated angles. Each intensity peak shows that X-rays satisfy Bragg's equation.³⁸ An X-ray powder diffractometer, a model named, Bruker D8 Advance diffractometer, brought from Bremen, Germany, was employed to record the XRD patterns of AgNPs using $\text{Cu } \alpha$ radiation as a source of X-rays with the wavelength of $\lambda = 1.5406 \text{ \AA}$. The obtained XRD patterns vary in the range of 20–80° of 2θ values, as displayed in Figure 5. The XRD pattern's peaks appeared at various 2θ values confirmed the synthesis of silver NPs in comparison to the reference graph [taken from the joint committee on powder

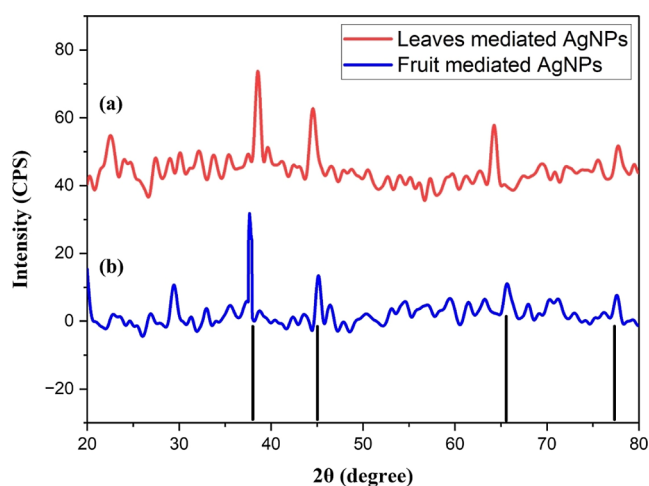


Figure 5. XRD pattern of *C. fistula*-mediated AgNPs for (a) leaf extract, and (b) fruit extract.

diffraction standards (JCPDS)], along with the confirmation of their crystallinity due to the sharpness of the peaks. These peaks demonstrated the *hkl* values of (111), (200), (220), and (311) at 2θ values of 38.7, 44.6, 66.7, and 77.65°, in a sequence, for leaf extracted-mediated AgNPs (see Figure 5a). However, the fruit extract-mediated AgNPs also provided the same planes, as displayed in Figure 5b with variations in 2θ values of 38.35, 45.4, 65.6, and 77.6°, respectively. These results confirmed the FCC structure of AgNPs, upon the comparison of patterns with JCPDS ID no. 04-0783 (black-colored reference graph).

The crystal lattice gets affected by strain, and instrumental adjustments can have an impact on peak width. FWHM (full-width half maximum) value, which is represented by β , was evaluated manually through the prominent peak of the XRD pattern and observed to be 0.0093 for leaf and 0.128 for fruit extract-mediated AgNPs. The lattice parameter was calculated using Bragg's law,³⁹ at the prominent peaks of *hkl* value (111) for both leaf and fruit extracts of *C. fistula*-mediated AgNPs, where we obtained the corresponding results as 0.39 and 0.41 nm, respectively. However, to analyze the crystallite size of the synthesized AgNPs, the Debye–Scherrer equation⁴⁰ was employed, and can be mathematically presented as

$$D = \delta\lambda / \beta \cos \theta \quad (2)$$

Table 1 illustrates the structural parameters of the synthesized NPs, which have a crystallite size of 16.9 nm for leaf extract-mediated NPs and 1.19 nm for fruit extract-mediated NPs, pointing to efficient compatibility with our approximated UV–vis results.

3.2. UV–Visible Spectroscopy Analysis. UV–visible spectroscopy technique is an efficacious method to examine

Table 1. Structural Parameters of *C. fistula* Leaf and Fruit Extract-Mediated AgNPs

samples	2θ (deg)	FWHM (β) (rad)	Miller indices	crystallite size (nm)	lattice constant (nm)
<i>C. fistula</i> leaf extract mediated AgNPs	38.7	0.0093	(111)	16.9	0.39
<i>C. fistula</i> fruit extract mediated AgNPs	38.35	0.128	(111)	1.19	0.41

the optical properties of colloidal NPs due to their property of having a very small band gap, wherein colloidal NPs give rise to different colors because of SPR absorption, determined by their size, shape, and so forth.^{41,42} Graphical data are shown, corresponding to wavelength and absorbance along the *x*- and *y*-axes which were obtained using a UV–vis spectroscopy model named Shimadzu UV-1800 (Japan).³³ Because of the specific wavelength and frequency of the incident photons (light), the SPR effect occurs with the interaction of photons with electrons on the surface of the material, and it excites the electrons by inducing plasmonic effects.⁴³ As displayed in Figure 6a,b, the UV–visible results provide a graphical display of leaf and fruit extract-mediated silver NPs, showing wavelength and absorbance along the *x*- and *y*-axes, respectively, whereas no peaks were observed for AgNO₃ precursor solution and leaf/fruit extracts; however, peaks at absorption values of 397 and 401 nm showed the presence of AgNPs. Moreover, the existence of spherical-shaped AgNPs was suggested by the single absorption peak. These particles were further investigated by SEM analysis.⁴⁴ Tauc's plot was drawn to compute the optical band gap of leaf and fruit-mediated nanosized particles by applying the equation⁴⁵

$$(\alpha h\nu)^{1/n} = A (h\nu - E_g) \quad (3)$$

wherein α denotes the coefficient of absorption, $h\nu$ denotes photon energy, A is taken as a proportionality constant, E_g represents the energy of the optical band gap, and n represents electronic transitions, wherein $n = 1/2$ shows the direct optical band gap transitions. Moreover, the $(\alpha h\nu)^2$ versus E_g graph, as displayed in Figure 6c, d, suggests the optical direct bandgap energy of AgNPs as 2.58 and 2.12 eV utilizing leaf extract (see Figure 6c) and fruit-pulp extract (see Figure 6d), respectively: these energies are compatible with the values in the existing literature, which are 2.9⁴⁶ and 3.4 eV.⁴⁷ The difference in the optical band gap energy values may be observed due to other phenomena, such as quantum confinement effects.⁴⁸

3.3. Morphological Analysis. For the consideration of the structures and anatomy of materials (mostly nanostructures), much versatile equipment is in use, including SEM.⁴⁹ A conductive medium for SEM analysis was provided by mounting the samples on double carbon tape, whereas the size of the crystallite was already calculated using the Debye–Scherrer formula. However, the morphological investigation was carried out to confirm the appearance of the leaf and fruit extract synthesized AgNPs by evaluating the SEM micrographs at 500 and 200 nm scales, as shown in Figure 7a.

The leaf extract synthesized AgNPs' SEM images (see Figure 7a) showed the agglomeration of particles due to the presence of biomolecules, which can be modified by frequent washing with distilled water, while fruit extract-mediated AgNPs (see Figure 7b) are well separated. This outcome is reported for the very first time and confirms the novelty of our research for featuring the smallest sized and well-dispersed green synthesized AgNPs which could have their potential applications in a range of medical research. The examination of *C. fistula* leaf extract synthesized AgNPs reported the diameter of the synthesized AgNPs between 50 and 80 nm, whereas fruit extract synthesized AgNPs were reported to lie between 12 and 20 nm, which illustrated their spherical shape. Various factors, including temperature, the pH level of the sample solution, total reaction time, and the concentration of extract and precursor solution, affect the shape of particles as

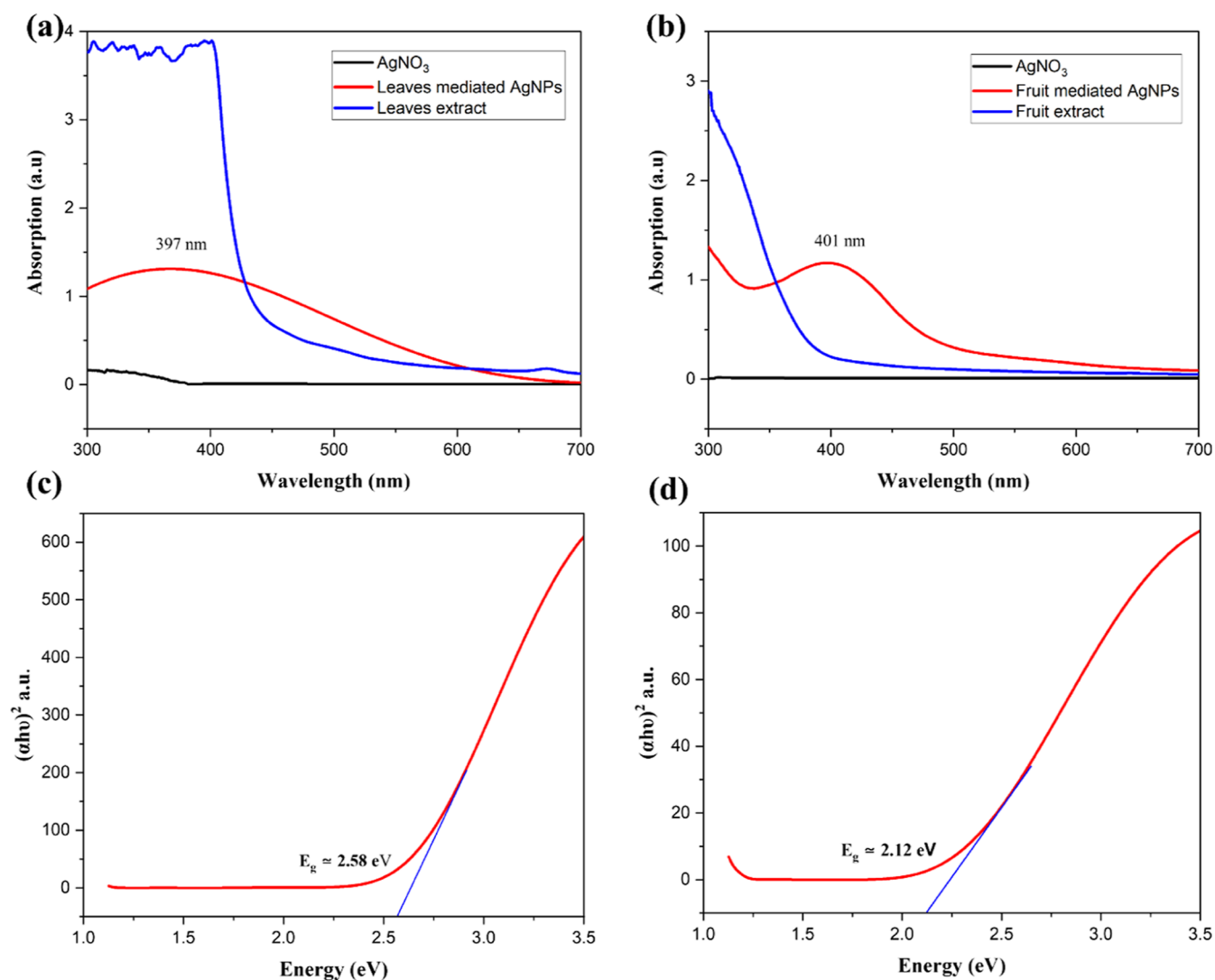


Figure 6. Absorption spectrum of UV–visible for as-synthesized AgNPs: (a) leaf extract and (b) fruit extract. Optical band gap of as-synthesized AgNPs: (c) leaf extract and (d) fruit extract.

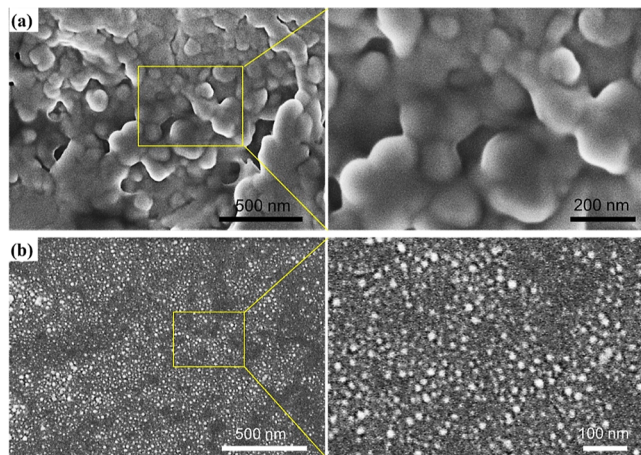


Figure 7. SEM images of *C. fistula*-mediated AgNPs synthesized from (a) leaf extract and (b) fruit extract.

well as their size; hence, regulating these parameters is considered an effective method to reduce the diameter of the synthesized NPs.⁵⁰ These NPs can be employed in biomedical

applications on the basis of their sizes, exploring their potential for imaging, antibiotics, and cancer treatment.⁵¹

The histogram in Figure 8 depicts the particle size distribution of as-synthesized AgNPs. For the *C. fistula* leaf extract-mediated AgNPs, the size was observed to be 40–120 nm; however, the maximum number of particles was in the 50–80 nm range (see Figure 8a). The increased particle size is owing to the agglomeration effects caused by biomolecules which reduced the surface area of the synthesized AgNPs, resulting in a larger size. On the other hand, *C. fistula* fruit extract-mediated AgNPs are smaller in size and are well dispersed in the range of 10 and 26 nm, with the maximum particle size in the 12–20 nm range (see Figure 8b).

3.4. Anti-Cancer Assay. The anti-cancer assay of *C. fistula* leaf and fruit extract synthesized AgNPs along with the extract itself was analyzed in the case of breast cancer cell lines (MCF-7) through the MTT assay, which is chemically 3-(4,5-dimethylthiazol-2-yl)-2,5-diphenyl tetrazolium bromide. The cell viability (%) with variations in concentration is presented in Figure 9. The cytotoxic effect of synthesized AgNPs on cancer growth cells was investigated at varying concentrations of 10–100 $\mu\text{g}/\text{mL}$. The percentage of cancer cell activity was shown to be affected by the plant extracts as well, along with

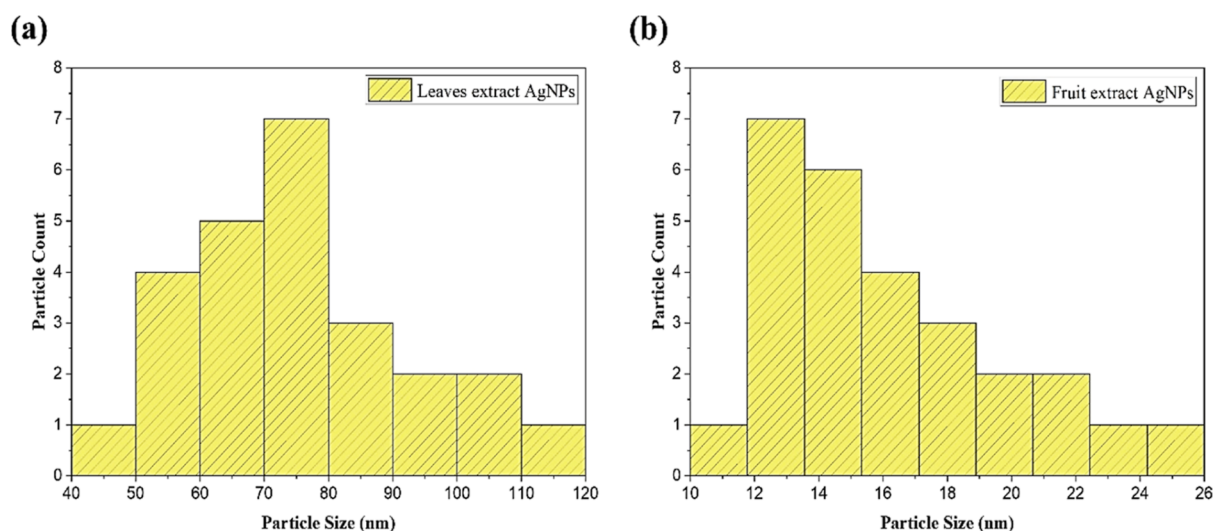


Figure 8. Particle size distribution of *C. fistula*-mediated AgNPs synthesized from (a) leaf extract and (b) fruit extract.

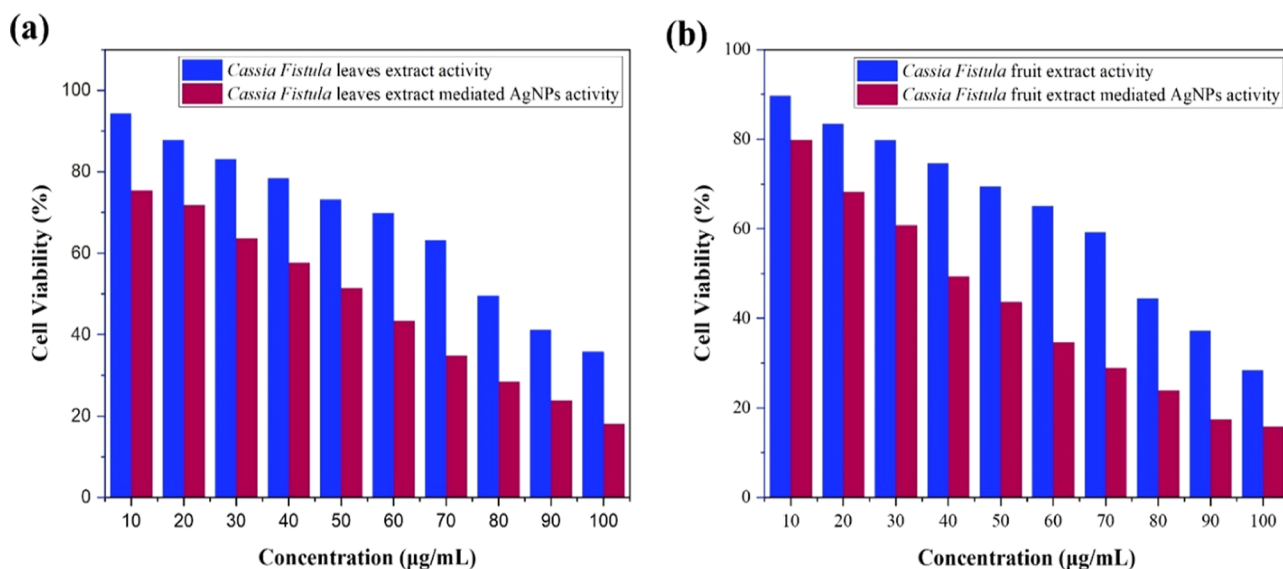


Figure 9. Anti-cancer (MCF-7) activity of (a) leaf extract and extract-mediated AgNPs and (b) fruit extract and extract-mediated AgNPs.

Table 2. Anti-Cancer (MCF-7) Activity of *C. fistula* Extracts and Their Mediated AgNPs at Varying Concentrations

C. fistula leaf extract		C. fistula leaf extract AgNPs		C. fistula fruit extract		C. fistula fruit extract AgNPs	
concentration (µg/mL)	% cell viability	concentration (µg/mL)	% cell viability	concentration (µg/mL)	% cell viability	concentration (µg/mL)	% cell viability
10	94.3	10	75.4	10	89.7	10	79.8
20	87.8	20	71.8	20	83.4	20	68.2
30	83.1	30	63.6	30	79.8	30	60.8
40	78.4	40	57.6	40	74.6	40	49.3
50	73.2	50	51.4	50	69.4	50	43.6
60	69.9	60	43.3	60	65.1	60	34.6
70	63.2	70	34.9	70	59.2	70	28.9
80	49.6	80	28.4	80	44.5	80	23.9
90	41.1	90	23.8	90	37.2	90	17.4
100	35.8	100	18.1	100	28.4	100	15.8

the extract-synthesized AgNPs, and this percentage was noted to increase with the increase in concentrations of both solutions. The maximum cell growth was found to be 18% at 100 µg/mL concentration in the case of *C. fistula* leaf extract-mediated AgNPs, while 36% for leaf extract at 100 µg/mL

concentration (see Figure 9a). On the other hand, the *C. fistula* fruit extract showed the highest effectivity of 28% cell growth at 100 µg/mL, while leaf extract-mediated AgNPs showed the maximum effectivity of 16% at 100 µg/mL concentration (see Figure 9b). This research demonstrates that both the extracts

and the extract-mediated AgNPs are effective for efficient anti-cancer treatment, wherein synthesized AgNPs were most efficient to stimulate reactive oxygen species (ROS) to damage the target cell components and cause cell death.⁵² Table 2 summarizes the anti-cancer (MCF-7) assay parameters for extracts and extracts-mediated AgNPs at varying concentrations.

3.5. Anti-Cancer Mechanism. It is well-known that most cancer cells exhibit an enhanced permeation and retention effect. This effect may allow the efficient interaction of silver NPs with cancer cells (see Figure 10). It results in the invasion

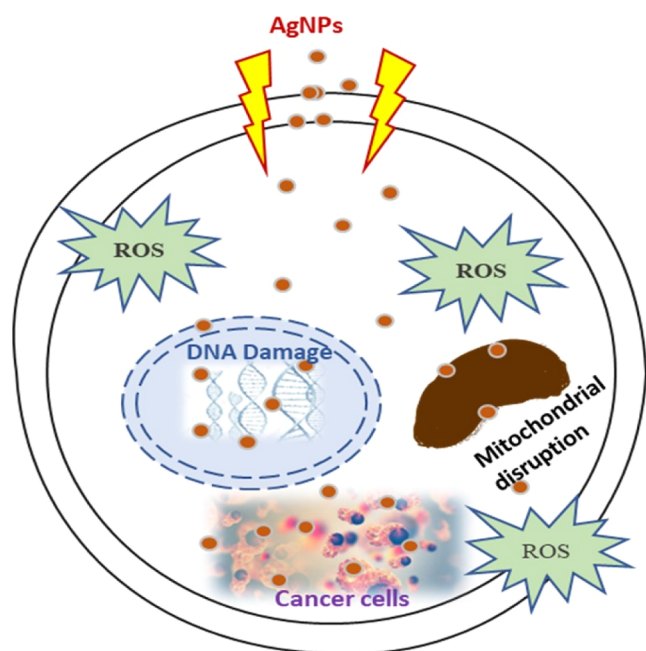


Figure 10. Possible anti-cancer mechanism of AgNPs.

and accumulation of many AgNPs followed by the death of cancer cells, and as a result, the uncontrolled division of cancer cells can be handled. Furthermore, AgNPs induce early apoptosis by modulating physiological signaling pathways.⁵³ Treating the cancer cells with silver NPs leaves them with significantly changed morphology, which may include cell shrinkage, shape irregularity, or blebbing cytoplasm. Changes in cancer cells may also be caused by ROS production, which causes oxidative stress and eventually leads the cell to die.⁵⁴ Oxidative stress, caused by ROS production in tumor cells, dismantles the vital biomolecules required for proper cell function, disrupting the various physiological processes and pathways, accompanied by the destruction of important cellular organelles and bio-membranes, and eventually causing tumor cell death.^{55,56}

4. CONCLUSIONS

C. fistula can reduce as well as stabilize the medium, which aids in producing metal NPs. By taking advantage of this property, we studied the biomedical efficacy of AgNPs by favorably preparing them using *C. fistula* leaf and fruit extracts based on a green synthesis technique. *C. fistula* extracts are rich in flavonoids, alkaloids, phenolic compounds, and other phytochemicals. These elements are responsible for the reducing properties of the extracts. The silver NPs mediated by leaf and fruit extracts were between 50–80 and 12–20 nm in size, with

an FCC crystal structure confirmed by XRD analysis and SEM investigations. Furthermore, the MCF-7 breast cancer cell line was used to examine the extracts and their synthesized AgNPs' anti-cancer assay, which was shown to be highly supportive in reducing tumor cell growth by increasing the concentrations of the solutions. We confirmed that the *C. fistula* fruit extract-mediated AgNPs have the highest activity of their counterparts and can be potentially used in biomedical applications..

■ ASSOCIATED CONTENT

Data Availability Statement

All data generated or analyzed during this study are included in this article.

■ AUTHOR INFORMATION

Corresponding Authors

Muhammad Aamir Iqbal – School of Materials Science and Engineering, Zhejiang University, Hangzhou 310027, China;
 orcid.org/0000-0002-5031-5305;

Email: maiqbal.research@gmail.com

Jeong Ryeol Choi – School of Electronic Engineering, Kyonggi University, Suwon, Gyeonggi-do 16227, Republic of Korea;
 Email: choiardor@hanmail.net

Authors

Rija Abaid – Centre of Excellence in Solid State Physics, University of the Punjab, Lahore 54590, Pakistan

Maria Malik – Centre of Excellence in Solid State Physics, University of the Punjab, Lahore 54590, Pakistan

Mariam Malik – Faculty of Biological and Applied Sciences, International Islamic University, Islamabad 04436, Pakistan

Zubeda Shahwani – Guangdong Key Laboratory for Genome Stability and Disease Prevention and Guangdong Key Laboratory for Biomedical Measurements and Ultrasound Imaging, Department of Biomedical Engineering, Shenzhen University, School of Medicine, Shenzhen 518060, China

Taha Zaid Ali – Pharmacy Department, Al-Mustaqbal University College, Babylon 51001, Iraq

Kareem Morsy – Biology Department, College of Science, King Khalid University, Abha 61421, Saudi Arabia

Rey Y. Capangpangan – Department of Physical Sciences and Mathematics, College of Marine and Allied Sciences Mindanao State University at Naawan, Naawan 9023 Misamis Oriental, Philippines

Arnold C. Alguno – Department of Physics, Premier Research Institute of Science and Mathematics (PRISM) Mindanao State University - Iligan Institute of Technology, Iligan City 9200, Philippines

Complete contact information is available at:

<https://pubs.acs.org/10.1021/acsomega.3c02225>

Author Contributions

♦R.A. and M.M. contributed equally and share the first authorship. R.A.: conceptualization, methodology, writing—original draft preparation, and validation. M.M.: conceptualization, resources, methodology, writing—original draft preparation, writing—review and editing, and validation. M.A.I.: conceptualization, writing—review and editing, and funding acquisition. M.M.: writing—review and editing and proofreading. Z.S.: reviewing and editing. T.Z.A.: reviewing and validation. K.M.: reviewing, validation, and funding. R.Y.C.: reviewing, proofreading, and validation. A.C.A.: reviewing, proofreading, and validation. J.R.C.: writing—review and

editing, proofreading, validation, and funding acquisition. All authors have read and agreed to the published version of the manuscript.

Notes

The authors declare no competing financial interest.

ACKNOWLEDGMENTS

The authors acknowledge the support provided by University of the Punjab, Pakistan. The authors also acknowledge the support provided by the National Research Foundation of Korea (NRF) grant funded by the Korean government (MSIT) (no.: NRF-2021R1F1A1062849) while extending their appreciation to the Deanship of Scientific Research at King Khalid University for supporting this work through large groups (project under grant number R.G.P.2/1/44).

REFERENCES

- (1) Acharya, A.; Kamilla, S. K.; Nayak, M. K.; Roy, G. S. Nano the revolution of 21st century. *J. Phys. Educ.* **2011**, *5*, 16.
- (2) Christian, P.; Von Der Kammer, F.; Baalousha, M.; Hofmann, T. Nanoparticles: structure, properties, preparation and behaviour in environmental media. *Ecotoxicology* **2008**, *17*, 326–343.
- (3) Iqbal, S.; Javed, M.; Bahadur, A.; Qamar, M. A.; Ahmad, M.; Shoaib, M.; Raheel, M.; Ahmad, N.; Akbar, M. B.; Li, H. Controlled synthesis of Ag-doped CuO nanoparticles as a core with poly (acrylic acid) microgel shell for efficient removal of methylene blue under visible light. *J. Mater. Sci.* **2020**, *31*, 8423.
- (4) Bahadur, A.; Saeed, A.; Shoaib, M.; Iqbal, S.; Bashir, M. I.; Waqas, M.; Hussain, M. N.; Abbas, N. Eco-friendly synthesis of magnetite (Fe₃O₄) nanoparticles with tunable size: dielectric, magnetic, thermal and optical studies. *Mater. Chem. Phys.* **2017**, *198*, 229–235.
- (5) Ndikau, M.; Noah, N. M.; Andala, D. M.; Masika, E. Green synthesis and characterization of silver nanoparticles using Citrullus lanatus fruit rind extract. *Int. J. Anal. Chem.* **2017**, *2017*, 1–9.
- (6) Shaik, M.; Khan, M.; Kuniyil, M.; Al-Warthan, A.; Alkhatlan, H.; Siddiqui, M.; Shaik, J.; Ahamed, A.; Mahmood, A.; Khan, M.; et al. Plant-extract-assisted green synthesis of silver nanoparticles using *Origanum vulgare* L. extract and their microbicidal activities. *Sustain. Sci.* **2018**, *10*, 913.
- (7) Li, S.; Shen, Y.; Xie, A.; Yu, X.; Qiu, L.; Zhang, L.; Zhang, Q. Green synthesis of silver nanoparticles using *Capsicum annuum* L. Extract. *Green Chem.* **2007**, *9*, 852.
- (8) Bai, H.; Zhang, Z.; Guo, Y.; Jia, W. Biological synthesis of size-controlled cadmium sulfide nanoparticles using immobilized *Rhodobacter sphaeroides*. *Nanoscale Res. Lett.* **2009**, *4*, 717.
- (9) Tho, N. T. M.; An, T. N. M.; Tri, M. D.; Sreekanth, T. V. M.; Lee, J.-S.; Nagajyothi, P. C.; Lee, K. D. Green synthesis of silver nanoparticles using *Nelumbo nucifera* seed extract and its antibacterial activity. *Acta Chim. Slov.* **2013**, *60*, 673–678.
- (10) Carmona, E. R.; Benito, N.; Plaza, T.; Recio-Sánchez, G. Green synthesis of silver nanoparticles by using leaf extracts from the endemic *Buddleja globosa* hope. *Green Chem. Lett. Rev.* **2017**, *10*, 250–256.
- (11) Sreekanth, T. V. M.; Duk Lee, K. Green Synthesis of Silver Nanoparticles from *Carthamus tinctorius* Flower Extract and Evaluation of their Antimicrobial and Cytotoxic Activities. *Curr. Nanosci.* **2011**, *7*, 1046–1053.
- (12) Burlacu, E.; Tanase, C.; Coman, N. A.; Berta, L. A review of bark-extract-mediated green synthesis of metallic nanoparticles and their applications. *Molecules* **2019**, *24*, 4354.
- (13) Lalithamba, H. S.; Raghavendra, M.; Uma, K.; Yatish, K. V.; Mousumi, D.; Nagendra, G. *Capsicum annuum* fruit extract: A novel reducing agent for the green synthesis of ZnO nanoparticles and their multifunctional applications. *Acta Chim. Slov.* **2018**, *65*, 354–364.
- (14) Al-Radadi, N. S. Green synthesis of platinum nanoparticles using Saudi's Dates extract and their usage on the cancer cell treatment. *Arabian J. Chem.* **2019**, *12*, 330–349.
- (15) Malik, M.; Aamir Iqbal, M.; Iqbal, Y.; Malik, M.; Bakhsh, S.; Irfan, S.; Ahmad, R.; Pham, P. V. Biosynthesis of silver nanoparticles for biomedical applications: A mini review. *Inorg. Chem. Commun.* **2022**, *145*, 109980.
- (16) Sridevi, H.; Bhat, M. R.; Kumar, P. S.; Kumar, N. M.; Selvaraj, R. Structural characterization of cuboidal α -Fe₂O₃ nanoparticles synthesized by a facile approach. *Appl. Nanosci.* **2023**, *16*, 1–9.
- (17) Vinayagam, R.; Hebbar, A.; Senthil Kumar, P.; Rangasamy, G.; Varadavenkatesan, T.; Murugesan, G.; Srivastava, S.; Concepta Goveas, L.; Manoj Kumar, N.; Selvaraj, R. Green synthesized cobalt oxide nanoparticles with photocatalytic activity towards dye removal. *Environ. Res.* **2023**, *216*, 114766.
- (18) Vinayagam, R.; Kandati, S.; Murugesan, G.; Goveas, L. C.; Baliga, A.; Pai, S.; Varadavenkatesan, T.; Kaviyarasu, K.; Selvaraj, R. Bioinspiration synthesis of hydroxyapatite nanoparticles using eggshells as a calcium source: Evaluation of Congo red dye adsorption potential. *J. Mater. Res. Technol.* **2023**, *22*, 169–180.
- (19) Sangeetha, G.; Rajeshwari, S.; Venckatesh, R. Green synthesis of zinc oxide nanoparticles by aloe barbadensis miller leaf extract: Structure and optical properties. *Mater. Res. Bull.* **2011**, *46*, 2560–2566.
- (20) Jayalakshmi, Y. A. Green synthesis of copper oxide nanoparticles using aqueous extract of flowers of *Cassia alata* and particles characterization. *Dig. J. Nanomater. Biostruct.* **2014**, *4*, 66–71.
- (21) Bahorun, T.; Neergheen, V. S.; Aruoma, O. I. Phytochemical constituents of *Cassia fistula*. *Afr. J. Biotechnol.* **2005**, *4*, 1530–1540.
- (22) Ahmad, N.; Sharma, S.; Alam, M. K.; Singh, V. N.; Shamsi, S. F.; Mehta, B. R.; Fatma, A. Rapid synthesis of silver nanoparticles using dried medicinal plant of basil. *Colloids Surf, B* **2010**, *81*, 81–86.
- (23) Panigrahi, S.; Kundu, S.; Ghosh, S.; Nath, S.; Pal, T. General method of synthesis for metal nanoparticles. *J. Nanopart. Res.* **2004**, *6*, 411–414.
- (24) Thirumal, M.; Srimanthula, S.; Kishore, G. *Cassia fistula* Linn-Pharmacognostical, phytochemical and pharmacological review. *Crit. Rev. Pharm. Sci.* **2012**, *1*, 43–65.
- (25) Modi, F. K.; Khorana, M. L. A study of *Cassia fistula* pulp. *Indian J Pharm*, *4*, 61-3., & Szentagali, I. A. *Cassia fistula* hat_anya. *Ber. Ung. Pharm. Ges.* **1937**, *13*, 61–63.
- (26) Duraipandiyam, V.; Baskar, A. A.; Ignacimuthu, S.; Muthukumar, C.; Al-Harbi, N. A. Anticancer activity of Rhein isolated from *Cassia fistula* L. flower. *Asian Pac. J. Trop. Dis.* **2012**, *2*, S517–S523.
- (27) Luximon-Ramma, A.; Bahorun, T.; Soobrattee, M. A.; Aruoma, O. I. Antioxidant activities of phenolic, proanthocyanidin, and flavonoid components in extracts of *Cassia fistula*. *J. Agric. Food Chem.* **2002**, *50*, 5042–5047.
- (28) Krishnaraj, C.; Jagan, E. G.; Rajasekar, S.; Selvakumar, P.; Kalaichelvan, P. T.; Mohan, N. Synthesis of silver nanoparticles using *Acalypha indica* leaf extracts and its antibacterial activity against water borne pathogens. *Colloids Surf, B* **2010**, *76*, 50–56.
- (29) Nozhat, Z.; Khalaji, M. S.; Hedayati, M.; Kia, S. K. Different methods for cell viability and proliferation assay: essential tools in pharmaceutical studies. *Anticancer Agents Med. Chem.* **2022**, *22*, 703–712.
- (30) Okafor, F.; Janen, A.; Kukhtareva, T.; Edwards, V.; Curley, M. Green synthesis of silver nanoparticles, their characterization, application and antibacterial activity. *Int. J. Environ. Res. Public Health* **2013**, *10*, 5221–5238.
- (31) Yasir, M.; Singh, J.; Tripathi, M.; Singh, P.; Shrivastava, R. Green synthesis of silver nanoparticles using leaf extract of common arrowhead houseplant and its anticandidal activity. *Pharmacogn. Mag.* **2017**, *13*, S840–S844.
- (32) Irvani, S. Green synthesis of metal nanoparticles using plants. *Green Chem.* **2011**, *13*, 2638.

- (33) Yusof, K. N.; Alias, S. S.; Harun, Z.; Basri, H.; Azhar, F. H. Parkia speciosa as Reduction Agent in Green Synthesis Silver Nanoparticles. *ChemistrySelect* **2018**, *3*, 8881–8885.
- (34) Johnson, L.; Prabu, H. J. Green synthesis and characterization of silver nanoparticles by leaf extracts of *Cycas circinalis*, *Ficus amplissima*, *Commelina benghalensis* and *Lippia nodiflora*. *Int. Nano Lett.* **2015**, *5*, 43–51.
- (35) Sujitha, V.; Murugan, K.; Paulpandi, M.; Panneerselvam, C.; Suresh, U.; Roni, M.; Nicoletti, M.; Higuchi, A.; Madhiyazhagan, P.; Subramaniam, J.; et al. Green-synthesized silver nanoparticles as a novel control tool against dengue virus (DEN-2) and its primary vector *Aedes aegypti*. *Parasitol. Res.* **2015**, *114*, 3315–3325.
- (36) Bunaciu, A. A.; Udriștițoiu, E. g.; Aboul-Enein, H. Y. X-ray diffraction: Instrumentation and applications. *Crit. Rev. Anal. Chem.* **2015**, *45*, 289–299.
- (37) Rajeshkumar, S.; Bharath, L. V. Mechanism of plant-mediated synthesis of silver nanoparticles – A review on biomolecules involved, characterisation and antibacterial activity. *Chem.—Biol. Interact.* **2017**, *273*, 219–227.
- (38) Barbara, L. D.; Christine, M. C. X-ray Powder Diffraction (XRD). Available online: https://serc.carleton.edu/research_education/geochemsheets/techniques/XRD (accessed on Sept 18, 2021).
- (39) Jauncey, G. E. M. The scattering of X-rays and Bragg's law. *Proc. Natl. Acad. Sci. U.S.A.* **1924**, *10*, 57–60.
- (40) Holzwarth, U.; Gibson, N. The Scherrer equation versus the 'Debye-Scherrer equation'. *Nat. Nanotechnol.* **2011**, *6*, 534.
- (41) Perkampus, H. H. *UV-VIS Spectroscopy and its Applications*; SBBM, 2013.
- (42) Amendola, V.; Bakr, O. M.; Stellacci, F. A study of the surface plasmon resonance of silver nanoparticles by the discrete dipole approximation method: Effect of shape, size, structure, and assembly. *Plasmonics* **2010**, *5*, 85–97.
- (43) Westcott, S. L.; Oldenburg, S. J.; Lee, T. R.; Halas, N. J. Formation and adsorption of clusters of gold nanoparticles onto functionalized silica nanoparticle surfaces. *Langmuir* **1998**, *14*, 5396–5401.
- (44) Raza, M. A.; Kanwal, Z.; Rauf, A.; Sabri, A. N.; Riaz, S.; Naseem, S. Size- and shape-dependent antibacterial studies of silver nanoparticles synthesized by wet chemical routes. *J. Nanomater.* **2016**, *6*, 74.
- (45) Feng, Y.; Lin, S.; Huang, S.; Shrestha, S.; Conibeer, G. Can Tauc plot extrapolation be used for direct-band-gap semiconductor nanocrystals. *J. Appl. Phys.* **2015**, *117*, 125701.
- (46) Thirumagal, N.; Jeyakumari, A. P. Structural, Optical and Antibacterial Properties of Green Synthesized Silver Nanoparticles (AgNPs) Using *Justicia adhatoda* L. Leaf Extract. *J. Cluster Sci.* **2020**, *31*, 487–497.
- (47) Abdalameer, N. K.; Khalaph, K. A.; Ali, E. M. Ag/AgO nanoparticles: Green synthesis and investigation of their bacterial inhibition effects. *Mater. Today: Proc.* **2021**, *45*, 5788–5792.
- (48) Das, A. J.; Kumar, R.; Goutam, S. P. Sunlight Irradiation Induced Synthesis of Silver Nanoparticles using Glycolipid Biosurfactant and Exploring the Antibacterial Activity. *J. Bioeng. Biomed. Sci.* **2016**, *06*, 5.
- (49) Zhou, W.; Apkarian, R.; Wang, Z. L.; Joy, D. Fundamentals of scanning electron microscopy (SEM). *Scanning microscopy for nanotechnology*; Springer, 2006; pp 1–40.
- (50) Dada, A. O.; Adekola, F. A.; Adeyemi, O. S.; Bello, O. M.; Oluwaseun, A. C.; Awakan, O. J.; Grace, F.-A. A. Exploring the Effect of Operational Factors and Characterization Imperative to the Synthesis of Silver Nanoparticles. *Silver Nanoparticles: Fabrication, Characterization and Applications*; IntechOpen, 2018.
- (51) Iqbal, M. A.; Malik, M.; Le, T. K.; Anwar, N.; Bakhsh, S.; Shahid, W.; Shahid, S.; Irfan, S.; Al-Bahrani, M.; Morsy, K.; Do, H. B.; et al. Technological Evolution of Image Sensing Designed by Nanostructured Materials. *ACS Mater. Lett.* **2023**, *5*, 1027–1060.
- (52) Naseer, F.; Ahmed, M.; Majid, A.; Kamal, W.; Phull, A. R. Green nanoparticles as multifunctional nanomedicines: Insights into anti-inflammatory effects, growth signaling and apoptosis mechanism in cancer. *Semin. Cancer Biol.*; Academic Press, **2022**, *86*, 310–324.
- (53) Almatroodi, S. A.; Alsahli, M. A.; Rahmani, A. H. Berberine: An Important Emphasis on Its Anticancer Effects through Modulation of Various Cell Signaling Pathways. *Molecules* **2022**, *27*, 5889.
- (54) Nishijo, K.; Hosoyama, T.; Bjornson, C. R.; Schaffer, B. S.; Prajapati, S. I.; Bahadur, A. N.; Hansen, M. S.; Blandford, M. C.; McCleish, A. T.; Rubin, B. P.; Epstein, J. A.; et al. Biomarker system for studying muscle, stem cells, and cancer in vivo. *FASEB J.* **2009**, *23*, 2681–2690.
- (55) Velidandi, A.; Dahariya, S.; Pabbathi, N. P.; Kalivarathan, D.; Baadhe, R. R. A review on synthesis, applications, toxicity, risk assessment and limitations of plant extracts synthesized silver nanoparticles. *NanoWorld J.* **2020**, *6*, 35–60.
- (56) Malik, M.; Iqbal, M. A.; Malik, M.; Raza, M. A.; Shahid, W.; Choi, J. R.; Pham, P. V. Biosynthesis and Characterizations of Silver Nanoparticles from *Annona squamosa* Leaf and Fruit Extracts for Size-Dependent Biomedical Applications. *J. Nanomater.* **2022**, *12*, 616.